The main results are split into the 3 areas of application HVTS- DCS and bidirectional converters.

HVTS

WP 1 / D.1

Final specifications, duties and responsibilities for HVTS are established, including the specifications of HVTS prototype, and the specifications of multi-objective design and optimization environment (WP1/D.1.b). UPB-LEA coordinated these activities and provided the required documents.

WP 2.1.1 / D.2.1.1 b

Compilation of resonant operated power electronic circuit topologies is executed. Since resonant converters are well-known to be appropriate topology for high voltage application, the series resonant converter, parallel resonant converter, LLC resonant converter, LCC resonant converter and LLCC resonant converter are taken into account for the topology compilation regarding investigation of steady-state characteristics, parasitic integration capability, soft-switching operation region, control characteristics and topology complexity.

After detailed investigations and comparison, conclusions can be drawn that: 1) series resonant converter shows limited voltage conversion ratio and poor control characteristics for light load situation; 2) parallel resonant converter has poor control characteristics for full load situation; 3) LLC resonant converter has limited operating region in over-resonance zero-voltage-switching (ZVS) region; 4) LCC resonant converter has wide operating region regarding variable output voltage, power and load range; a well designed LCC resonant converter enables integration of the parasitics of transformer and multiplier circuit; LCC converter has an inherent short circuit protection; 5) compared with LCC resonant converter the more complex LLCC resonant converter has similar steady-state characteristics and operating region, the preferable local reactive power compensation capability unfortunately cannot be adopted for HVTS application; the suggestion of selecting the resonant frequency as the only operating point (e.g. f_{sn}=1) is infeasible, since the harmonics in the resonant current cannot be eliminated and the resulting increasing of n (transformer turns ratio) and k (CW stage number) are not preferable for HVTS application.

In summary, the LCC resonant converter has clearly turned out to be the most appropriate topology for HVTS application.

WP 2.1.2 a / D.2.1.1 a

An equivalent circuit of an ideal and real loaded high voltage multiplier rectifier circuit named Cockcroft-Walton (CW) or Greinacher cascade is derived from power electronics point of view. The corresponding loss model is built, which takes the influence from the boosting and smoothing capacitances, transformer resistance and diode dynamic resistance, diode forward voltage drop and stray capacitances into account.

The equivalent circuits of an ideal and real loaded three-stage (k=3) CW-multiplier are shown below, respectively. The input voltage of CW-multipliers are $U_p\ cos(\omega_s t)$, among which U_p is the amplitude of the quasi-sinusoidal output voltage from the resonant tank, ω_s is the switching frequency. n is the voltage turns ratio of the high voltage transformer, k is the stage number of the CW-multiplier. U_o is the specified output voltage of the CW-multiplier. C_{si}, C_{gi} (i=1,...k) are boosting and smoothing capacitance for each stage. D_{igs}, D_{isg} (i=1,...k) are ideal diodes between boosting and smoothing route for each stage with conducting direction from smoothing to boosting, or boosting to smoothing, respectively.

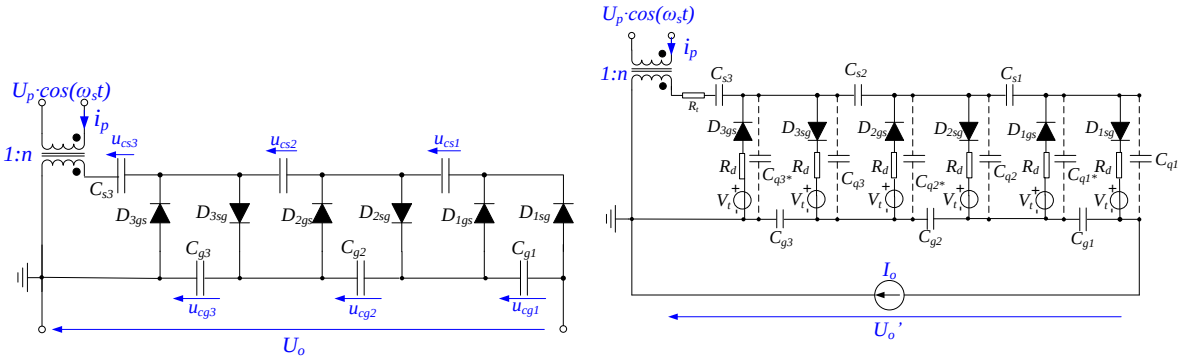

Equivalent circuit of (left) an ideal and (right) a real loaded HV CW multiplier

WP 2.1.2 b, c, d, e / D.2.1.1 b, D.2.2.1 a, b

The large-signal model of the LCC resonant converter adopting generalized averaging method and extended describing functions are derived. The verification through simulation and the steady-state characteristics regarding normalized switching frequency f_{sn} and duty cycle d are shown below, respectively.

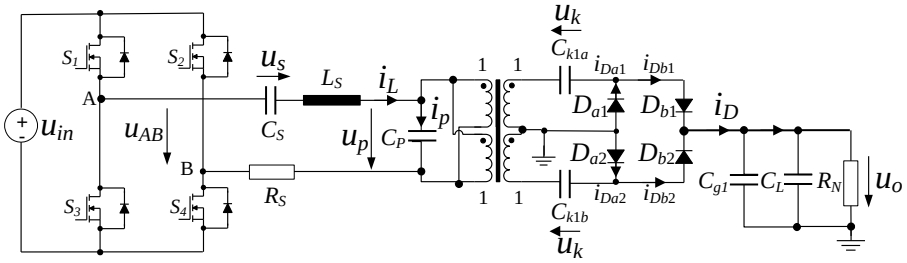

Circuit diagram of simplified LCC resonant converter

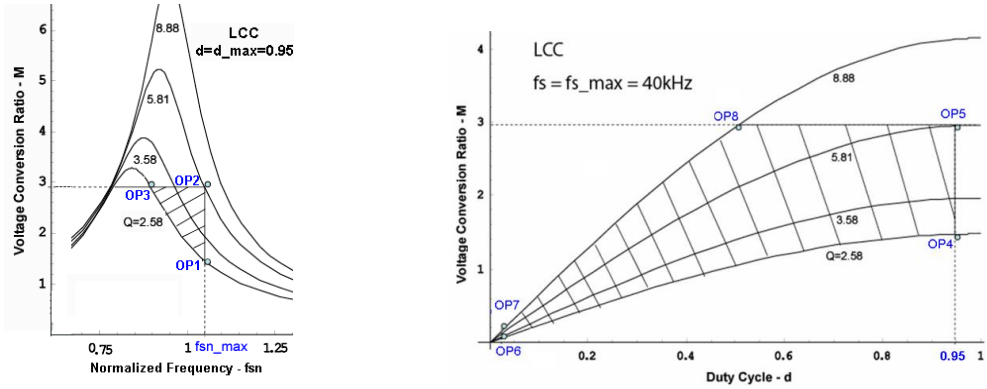

Voltage conversion ratio of LCC resonant converter vs. (left) normalized f_s and (left) duty cycle d

The component stress depends on the specified operating point and resonant parameters. Figures below show the relationship between resonant capacitor's ratio $\left(\frac{C_g}{C_p}=\frac{C_s}{C_p+C_s}\right)$ and the component stress with same operating point. It is obvious that larger resonant capacitor's ratio results in lower component stress for the same operating point.

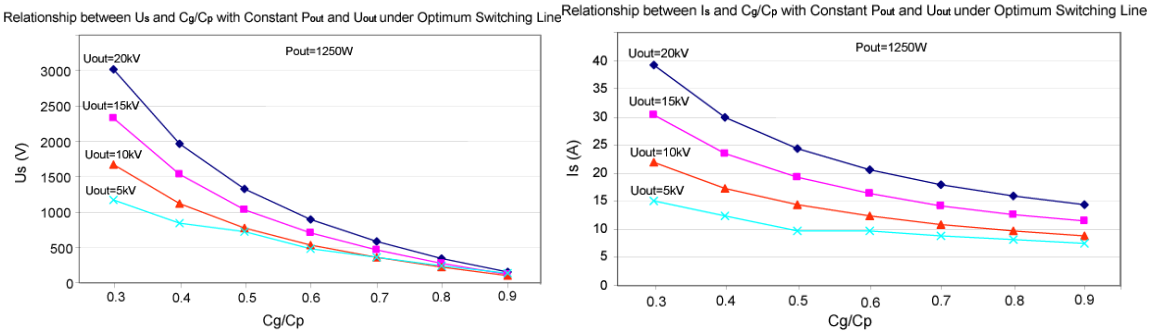

Relationship between component stress and resonant capacitor's ratio with the same output power or same output voltage under optimum f_s-d combination line (U_s is the peak value of the voltage across series capacitor C_s, I_s is the peak value of the resonant current through series inductor L_s, C_p is the parallel capacitor)

The loss model of the LCC resonant converter consists of four parts, such as full-bridge inverter, CW multiplier circuit, magnetic components (AC inductor L_s and HV transformer), and series capacitor C_s. In summary, they are briefly described below:

- Loss model of full-bridge inverter under optimum f_s-d combination:

  $$P_{FB}=4\cdot R_{DSon}\cdot {I_{Mrms}}^2+4\cdot(V_F\cdot I_{Davg}+R_D\cdot {I_{Drms}}^2)+2\cdot P_{SW}$$

  Among which, I_{Mrms} is the rms-current flowing through transistor, I_{Drms} and I_{Davg} is the rms and average current flowing through the parallel diode, R_{DSon} is the transistor´s on- resistance and R_D is the forward resistance of the diode, V_F is the diode forward voltage, and P_{sw} is the switching loss of the transistor.

- Loss model of CW multiplier circuit normally indicates the voltage drop in CW multiplier, which depends on the output current I_o, boosting and smoothing capacitors, switching frequency f_s, and stage number k. As an approximation, the voltage drop U_{CW_drop} can be represented as (C is the equivalent capacitor for boosting and smoothing route):

  $$U_{CW\_drop}\approx\frac{I_o}{C\cdot f_s}\cdot\left(\frac{2}{3}k^3+k^2-\frac{k}{12}\right)$$

- Loss model of series capacitor C_s. where tanδ is the capacitor´s loss factor.

$$P_{Cs} = \left(\frac{\sqrt{U_{ss}^{\ 2} + U_{sc}^{\ 2}}}{\sqrt{2}} \right)^2 \cdot \omega_s \cdot C_s \cdot \tan\delta = \frac{I_{Lp}^{\ 2} \cdot \tan\delta}{\omega_s \cdot C_s}$$

- Loss model of magnetic components, such as AC inductor L_s and HV transformer, is derived according to basic magnetic knowledge. The following three aspects are considered: core loss P_{fe}, low frequency copper loss P_{cu} and incremental effect due to skin and proximity effect in high frequency high current application.

$$P_{fe} = K_{fe0} \cdot f_s^{\ \xi} \cdot \Delta B^{\beta} \cdot A_c \cdot l_m$$

$$P_{cu} = \frac{\rho \cdot \lambda_1^{\ 2} \cdot I_{tot}^{\ 2} \cdot MLT}{4 \cdot K_u \cdot W_A \cdot A_c^{\ 2} \cdot \Delta B^2}$$

- Loss model of the series capacitor C_s. where tanδ is the capacitor loss factor.

$$P_{Cs} = \left(\frac{\sqrt{U_{ss}^{\ 2} + U_{sc}^{\ 2}}}{\sqrt{2}} \right)^2 \cdot \omega_s \cdot C_s \cdot \tan\delta = \frac{I_{Lp}^{\ 2} \cdot \tan\delta}{\omega_s \cdot C_s}$$

WP 2.1.2 f, WP 2.1.3 / D.2.1.1 c

Based on the derived large-signal model and loss model of LCC resonant converter, a computer aided design and optimization (CAD & CAO) environment is developed in CAMEL-VIEW-MOPO (iXtronics Co.). Since resonant current amplitude I_{LP} and voltage drop in CW multiplier U_{CW_drop} are critical variables, which determines the component stress, losses and indicates the wasteful cost, both of them are selected as the optimization objectives. The resulting multi-objective optimization process is shown below.

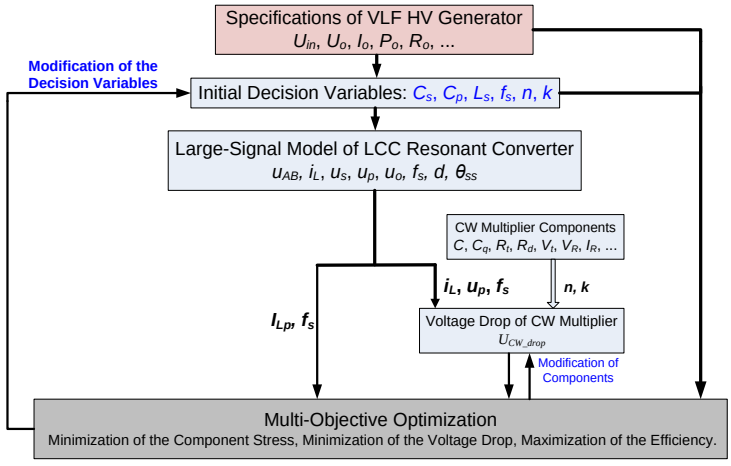

Multi-objective optimization procedure of LCC resonant converter

Through resonant parameters study, the graphical results regarding decision variables and Pareto front regarding two-objectives are obtained, as shown below. For such research, the transformer turns ratio *n* and CW multiplier stage number *k* are fixed through preliminary study.

Such CAD and CAO environment can be directly adopted by customer (e.g, BAUR Co.) and are beneficial for product performance improvement, cost reduction, and time to market.

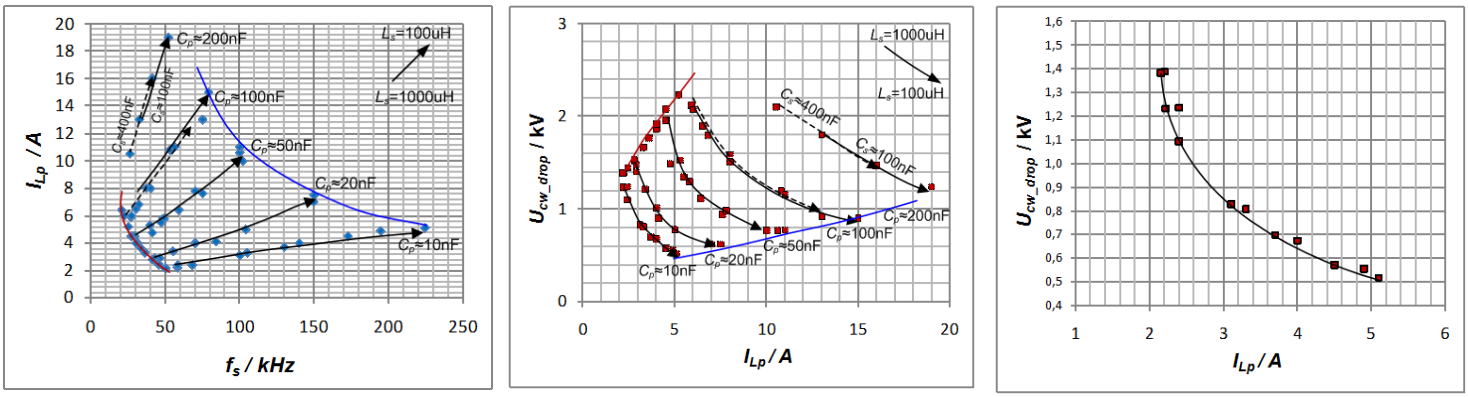

Graphical results, two dimensional illustration and Pareto front of LCC resonant converter in decision variables' range: C_s=100-800 nF, C_p=10-220 nF, L_s=100-1000 µH, n=7, k=2

WP 2.1.4 / D.2.1.2

After study of five different single units of multiplier circuits: 1) classical asymmetrical CW multiplier, 2) classical symmetrical CW multiplier, 3) simplified symmetrical CW multiplier, 4) Delon circuit and 5) bipolar CW multiplier, the simplified symmetrical CW multiplier, Delon circuit and bipolar CW multiplier circuit turned out to be the appropriate units for compact HVTS, since they need less components and show better steady-state and dynamic characteristics compared with the classical CW multiplier circuits. And these three kinds of multiplier circuits are further considered for the compact modular structure HVTS.

Through the study of multi-module series-connected multiplier circuits, which is potentially applicable for high voltage application, the following conclusions are drawn:

- 1) Modular structure HVTS consisting of simplified symmetrical CW generator has lower transformer stress, but higher capacitance stress;
- 2) Modular structure HVTS consisting of Delon circuit has higher transformer stress, but lower capacitance stress;
- 3) Modular structure HVTS consisting of bipolar CW generator shows medium transformer stress and capacitance stress;
- 4) Diodes stress of all three types of modular circuits are the same.
- 5) The output voltage in series-connected modular circuit is *m* (modular number) times of that in the single unit.

Through the study of multi-module parallel-connected multiplier circuits, which is potentially applicable for high power application the following conclusions can be drawn:

- 1) The component stress in parallel-connected modular circuit is the same as that in the single unit;
- 2) The output current in parallel-connected modular circuit is *m* (modular number) times of that in the single unit.

WP 2.2.1 / D.2.2.1

Based on the large-signal model, the linearized small-signal model of the LCC resonant converter is derived and experimentally verified.

Below shown are the small-signal equivalent circuit model of LCC resonant converter and the experimental verification results of control-to-output transfer functions.

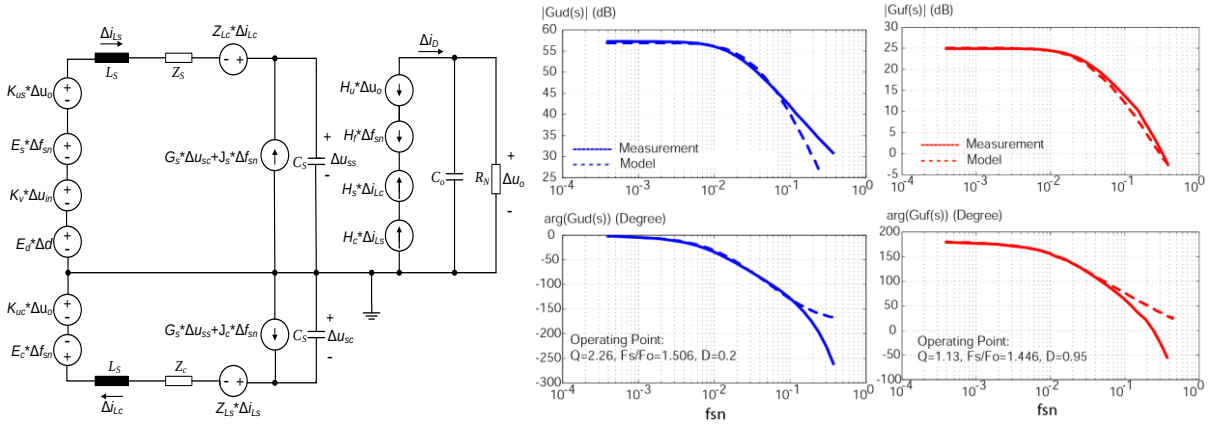

Small-signal equivalent circuit model of LCC resonant converter and experimental verification of control-to-output transfer functions comparison: (blue) control variable is d. f_s=40kHz, (red) control variable is f_s. d=0.95.

WP 2.2.2 / D.2.2.2

Based on the small-signal model and the analysis of dynamic characteristics, a cascaded two closed-loop control is developed. The inner is a current-mode control for regulating the resonant current. Three kinds of controllers are investigated: conventional linear PI controller, fuzzy PD controller and model-based fuzzy controller. For the outer loop a conventional PI controller serves for output voltage regulation. Simulated results in a small operating region are provided below. For a large operating region, it is expected that the fuzzy PD and model-based fuzzy control show superior behavior compared with the linear PI controller. Because of space limitation, the experimental verification on the scaled-down prototype is not given here.

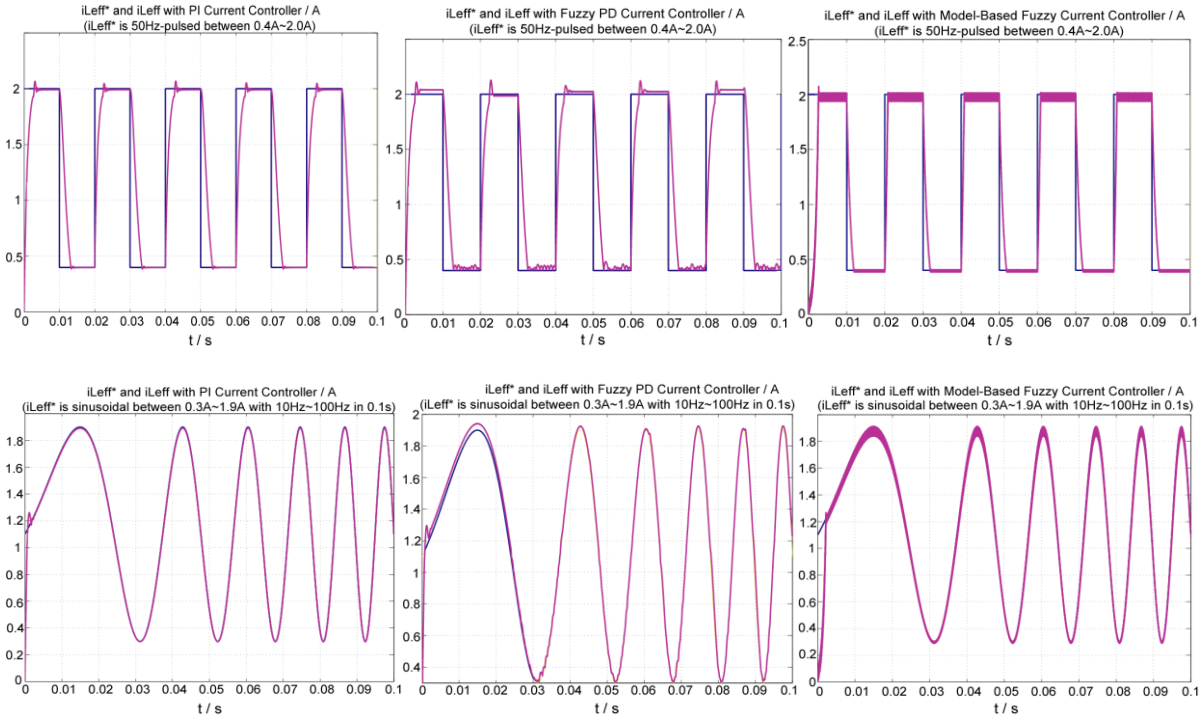

Simulated results of current-mode controller with square-wave or sinusoidal reference: (left) with PI controller; (middle) with fuzzy PD control; (right) with model-based fuzzy control.

From above given results the following conclusions are drawn:

- Linear PI current-mode controller has acceptable control performance considering the settling time, overshoot and steady-state error.
- Fuzzy PD controller has an obvious steady-state error, but it can be avoided using an adaptive gain in large operating region.
- Compared with linear PI controllers, model-based fuzzy controller has no overshoot, shorter settling time and it shows better performance in large operating regions.

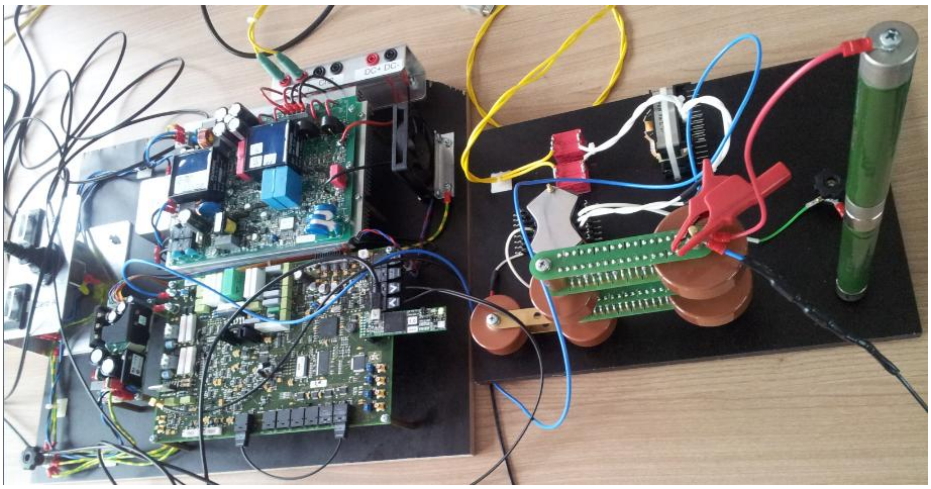

Photography of scaled-down HVTS prototype

WP 2.4 / D.2.4

Analogue R-controller concept and its small-signal model and corresponding dynamic characteristics based on a given operating point are studied. In order to get a sinusoidal output voltage, the R-controller consisting of series-connected transistors is adopted and operated as an electric load for discharging the output voltage.

According to the datasheet of the selected transistor and specified operating point, the capacitances, transconductance of the transistor are known. Referring to unified transistor model and Miller's theorem, an equivalent small-signal circuit model is derived. A cascaded two closed loop control is built for such model and executed in MATLAB-PLECS, bode plots and corresponding dynamic characteristics are obtained.

Reliability of analogue R-controller is also discussed, but such research should base on an experimental test or enough field data, which is not available at BAU. Supplementary work on the R-controller concentrates on the appropriate transistor selection, optimal number of series connected transistor determination.

DCS

Overview and Objectives

Due to the soft switching characteristics and the possibility to utilize parasitics of components and circuit resonant operated power supplies enable higher dynamic performance and efficiencies at light to medium loads. These properties qualifies them to be applied at todays requirements. However, in comparison with standard pulse width modulation (PWM) converter design and optimization of resonant converters are more complex. Especially for small and medium size enterprises (SMEs) it is very difficult to carry out optimal designs for resonant converters without a development environment.

Hence, a major objective of this project is to establish such a **development environment**. Under this development environment computer-aided steady-state and dynamic analysis for selected converter topologies can be performed. In combination with MOPO the power circuit and control parameters are designed and optimized.

The 2nd main objective is to apply this development environment to develop a new generation of DC source with higher dynamics and high efficiency based on resonant converter, incl. topological pre-selection, design and optimization of pre-selected converter topologies. Final decision is made utilizing a model-based topology comparison. A demonstrator is finally built to validate models in the development environment and experience the latter.

Development environment

Over view of the development environment

As shown in Fig. 1 four fundamental function modules are involved in the development environment:

- Steady-state analysis
- Dynamical analysis (large-signal and small-signal analysis)
- Semiconductor loss analysis
- Model-based converter design and optimization

Besides those fundamental modules two auxiliary modules for visualization and comparison are developed.

For each particular converter topology and its operation condition (incl. parameters, operation point) the electrical steady-state and dynamical characteristics are calculated firstly. The calculated electrical values (e.g. mean and RMS current through transistors and diodes, instant current and voltage at turn-on and turn-off instance, etc.) are input to semiconductor losses models. All computation results can be saved and visualized by the visualization module. Objective function can be built from those computational results and input to the multi-objective parameter optimization tool MOPO, which optimizes the converter parameters numerically using quasi Newton method. It should be noted that the optimization results are strongly depending on the selection of objective function. However, sometimes it is not so easy to decide which objective function suits best the individual design requirement. Hence, a comparison module for comparing specified characteristics (e.g. switching frequency, semiconductor losses, etc.) of different designs or different converter topologies is provided in this development environment.

All function blocks are implemented in M-language under MATLAB. Modular and extensible structures are applied to ensure the maintainability and extensibility of the development environment.

Implemented converter models

Within this project steady-state, dynamical and semiconductor loss models for standard 2-level phase-shifted full bridge (2L-PSFB), 3-level phase-shifted half bridge (1P3L-PSHB), 3-phase 3L-PSHB (3P3L-PSHB), series-parallel resonant converter with LC output filter (SPRC-LC) and 2-stage bidirectional solution with series resonant converter and buck-boost converter in triangular current mode (SRC-BBC) are developed according to the following state-of-the-art modeling techniques:

- For PWM converters:
  - Steady state models: current balancing of inductors and voltage balancing of capacitors
  - Dynamical models: state space average
- For resonant converters:
  - AC fundamental analysis and extended AC fundamental analysis
  - Extended describing function (EDF) method
- Semiconductor loss models:
  - Conduction losses: interpolation of linearized output characteristic of IGBT and forward characteristic of diodes at particular junction temperatures
  - Switching losses: look-up table (LUT) using instant current and voltage at switching actions for hard switching, neglecting soft switching losses, rough calculation of losses by hard switching with regenerative snubber by using a loss reduction factor

Model-based converter design under this development environment

The main objective of this work block is to develop a new generation of DC source (DCS) with higher dynamics under this development environment. . This work block is performed in two phases:

- Model-based converter design and comparison
- Small-signal analysis and control design

Model-based converter design and comparison

Comparison and selection of topology for a specific application is one of the most critical works for power converter development. Unfortunately this work is mostly done through a qualitative comparison based on experiences of engineers and/or published references. This comparison is usually efficient for a topology pre-selection, but not sufficient for a final decision, because a successfully applied converter topology in one particular case does not mean that it is also the best solution in another one. For a final decision a quantitative comparison is required in a rigorous design procedure.

Before a quantitative comparison all candidate converter topologies shall be designed and optimized according to an identical objective, in order to achieve a fair comparison. For simple converter topologies, e.g. hard switched PWM converters, their design and optimization is relatively easy using manual or simulative approach. For resonant converters, due to its design complexity a CAD-approach In conjunction with a numerical multi-objective multi-parameter (MOMP) optimization is required. This optimization cannot be performed based on simulations, because such simulations of are too time-consuming. Hence, an analytical model-based converter design, optimization and comparison are required.

Step 1: Pre-selection of converter topologies and strategies for operation

This critical stage is initiated by an analysis of technical requirements and current solution, the latter serving as reference. Limitation and drawbacks of the current solution and improvement potential through applying new circuit topologies and/or new operation strategies are studied.

Partner REG requires higher dynamic performance compared to the reference solution, good efficiency and power density. The boundary condition resulting from DCS-applications is the extreme wide operation range of $U_{out} = 0 \dots U_{rat}$ and $I_{out} = 0 \dots I_{rat}$ (s. Fig. 6). In order to achieve higher dynamics the determining output filter must be reduced by increasing the switching frequency or using interleaving technique. Unfortunately using the current 2L-PSFB topology it is not possible to increase the switching frequency without loss in efficiency, because zero voltage switching (ZVS) is lost at light load conditions and regenerative snubbers cannot be employed for the lagging leg. The reduction of switching losses is thus a major objective for topology selection.

The first possible topology is 1P3L-PSHB, which operates identically like the 2L-PSFB. Due to its 3-level structure IGBTs with lower reverse voltage can be employed and turn-off losses can be reduced. However, due to the doubled current conduction losses are increased. The question arrises, whether the increased conduction losses can be completely compensated by the reduced switching losses even at a higher switching frequency?

The second possible solution is to apply interleaving technique, e.g. 3P3L-PSHB. Since the filter frequency is three times the switching frequency it is possible to reduce the output filter without increasing the switching frequency. Another advantage of this topology is that the current of each phase is only one third of 1P3L-PSHB, which reduces the overall semiconductor conduction losses. Disadvantage of this variant is the more complex power circuitry (power electronics, transformer, etc.) and much higher installed semiconductor apparent power, yielding higher costs.

A completely different solution is the use of resonant converters. A pre-comparison of steady-state control characteristics yields the SPRC-LC as the most qualified among different resonant converter topologies. Due to its ZVS character in the total operation range the switching losses can be strongly reduced, especially if regenerative snubbers are employed for reducing the switch-off losses. Compared to 3P3L-PSHB the power circuit of SPRC-LC is much simpler. However, a big challenge of classical frequency-controlled (duty cycle equals one) SPRC-LC in this particular application is the extreme wide operation range, which implies a very large variation of switching frequency is required. If we use duty cycle control (at fixed switching frequency) ZVS condition cannot be ensured in the total operation range. Hence the questions arise: Can this critical problem be solved by an optimized modulation strategy? And can the known disadvantage of a relative higher amplitude of the primary current, which increases the conduction losses be compensated by the reduced switching losses even at a higher switching frequency?

Obviously all those questions listed above cannot be answered by performing a qualitative comparison. A model-based quantitative comparison is required for a final topology selection.

Step 2: Model-based converter design and comparison

For a quantitative comparison both PWM converters (1P3L-PSHB and 3P3L-PSHB) are designed to operate at the same switching frequency (20 kHz) as the reference 2L-PSFB. Parameters of passive components and semiconductor switchers are designed according to the technical specification (s. Table 1).

The SPRC-LC is designed using analytical models of the development environment. The worst case for the converter design is maximum output power fed by a minimal input DC voltage. Hence, the following objectives are considered in the converter design and optimization:

a) The converter can operate in the whole operation range by a minimum input voltage of $U_{dc} = 510\ \mathrm{V}$. Two critical operation points are (P_{rat}, U_{rat}) and (P_{rat}, I_{rat}), which are checked in the optimization routine.
b) Minimize the semiconductor losses and resonant current stress.
c) Maximize the switching frequency for achieving the higher dynamics requirement.

Since b and c are conflicting objectives a trade-off optimization shall be conducted. The optimized converter parameters are shown in Table 2.

As a SPRC-LC can be controlled both by switching frequency and duty cycle, we obtain an additional freedom to achieve a better steady-state and dynamical characteristics through optimizing the modulation strategy. As shown in Fig. 3 compared to the classic frequency modulation we can achieve ZVS in one leg and zero current switching (ZCS) in the other leg by using optimized modulation strategy. Hence, the switching losses of ZCS-leg and the turn-on loss of ZVS-leg can be almost eliminated. Since the ZVS switching condition in ZVS-leg can be ensured by a special state machine implemented in a field programmable gate array (FPGA), the turn-off loss of ZVS-leg is also strongly reduced by employing purely capacitive snubbers. As shown in Fig. 4 a switching frequency range of about 45 kHz to 210 kHz is required by using classic frequency modulation, which is unrealistic for practical implementation. While by using optimized modulation only a switching frequency range of about 40 kHz to 90 kHz is required. Another advantage of the optimized modulation strategy is the reduction of resonant current and semiconductor loss (s Fig. 4). Hence, optimized modulation strategy is selected as key feature for our application.

After design and optimization of all candidate topologies a model-based comparison is performed under the development environment. Comparison results show that SPRC-LC has low semiconductor losses and low RMS resonant current even at much higher switching frequency (s Fig. 4 and Fig. 5).

Step 3: Final power circuit design

In the final power circuit design the parameters are slightly adopted considering the component availability. After parameter adaptation converter characteristics are checked again using the development environment and analyzed in more detail using simulation tool PLECS.

Innovative dynamical modeling and control design for SPRC-LC

By developing a dynamical model for SPRC-LC (s. Fig. 2) it turned out that the classical EDF method according to E. X. Yang shows a large deviation, if the voltage across C_p is discontinuous. The reason is that the standard EDF method assumes all current and voltage waveforms of the resonant tank to be sinusoidal. As shown in Fig. 10 in continuous C_p voltage mode (CVM) all current and voltages in resonant tank are of nice sinusoidal shape. However, in discontinuous C_p voltage mode (DVM) the voltage across C_p strongly deviates from the sinusoidal shape. Results in design optimization show that in order to reduce reactive power, resonant current and switching losses a large part of the operation range should be operation in DVM (s. Fig. 6).

In order to solve this problem and to describe the dynamical behaviors more accurately, a novel EDF model for SPRC-LC is developed. Here the voltage on C_p is not assumed to be sinusoidal and is not considered as an independent state variable, but a function of i_{Ls} and i_{Lout}. Instead of an approximated output voltage, in the novel model it is calculated by the real voltage waveform across C_p, which is suitable for CVM, boundary condition and DVM. Simulative comparison results show a big deviation of the classical EDF model and a very good agreement of the novel EDF model (s. Fig. 7).

Perturbing the novel large-signal model at steady-state operation a small-signal model is deduced. Control parameters are design and optimized using classic loop gain method in the frequency domain. Due to the strong nonlinearity of the SPRC-LC gain a scheduling method is adopted for control parameter adaptation.

Prototyping and validation

Based on a SPRC-LC demonstrator (s. Fig. 9) analytical models of the development environment are validated. As an example the validation of the control characteristic is given in Fig. 9, which shows a very good agreement. Optimized modulation is realized in both operation modes (s. Fig. 10).

Conclusion and outlooks

Within this project a model-based development environment for converter design, optimization and comparison was developed, which was successfully applied in developing a new generation of DC sources. The major requirements of higher dynamics and high efficiency are achieved. However, due to the increased serial inductance volume and weight of magnetic components are higher than the current solution. In order to improve its economical efficiency methods for optimization of magnetic component shall be investigated in the future.

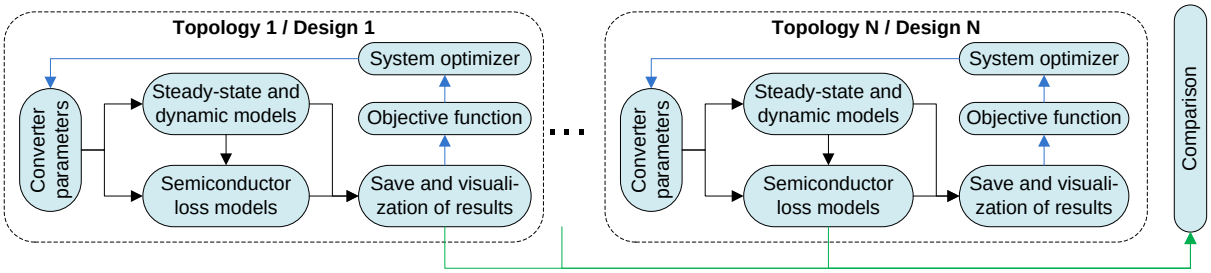

Fig. 1: Function blocks of development environment

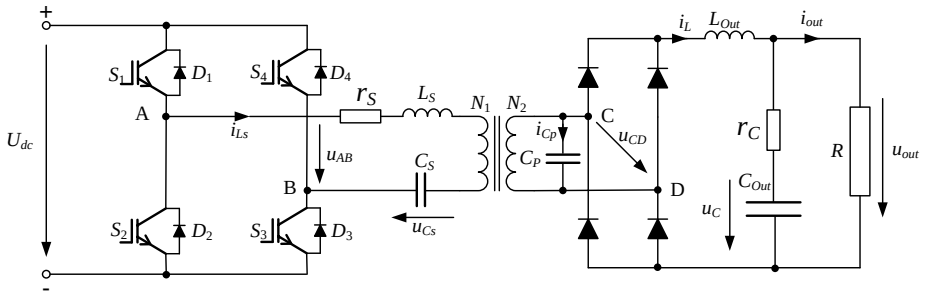

Fig. 2: Circuit diagram of SPRC-LC

Table 1: Converter parameters of 2L-PSFB, 1P3L-PSHB and 3P3L-PSHB

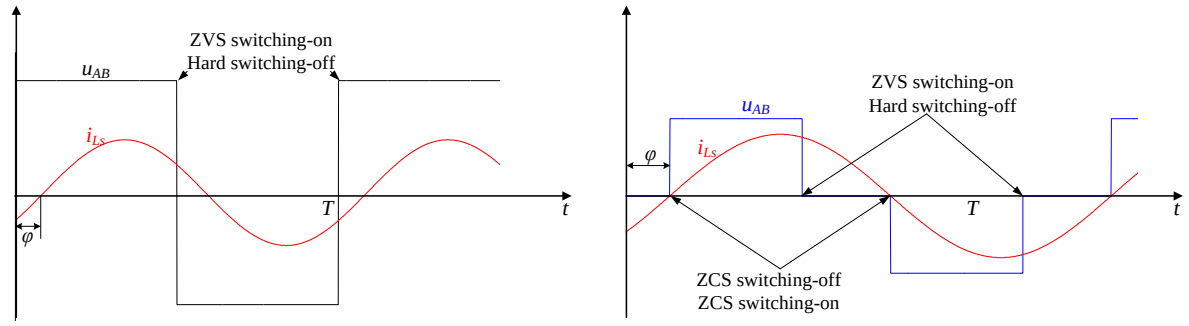

Fig. 3: Waveforms of SPRC-LC by using classic frequency modulation (link) and optimized modulation (right)

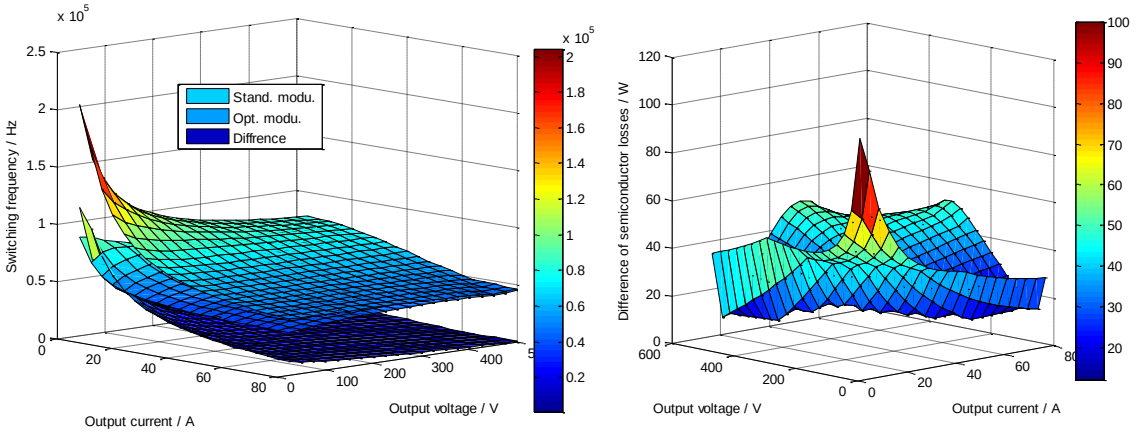

Fig. 4: Switching frequency (link) and difference semiconductor loss of SPRC-LC by using classic and optimized modulation strategies ($U_{dc} = 510$ V)

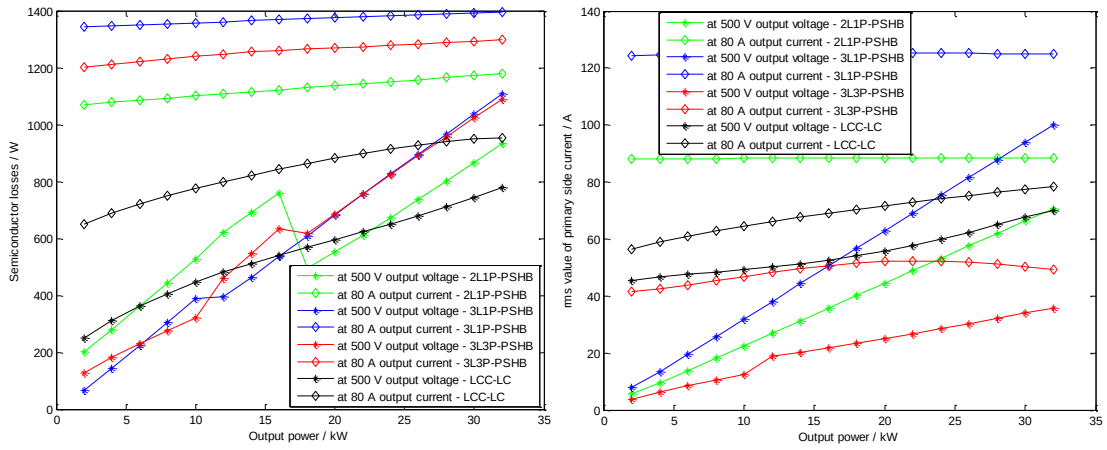

Fig. 5: Semiconductor loss (link) and primary side current (right) of difference candidate topologies

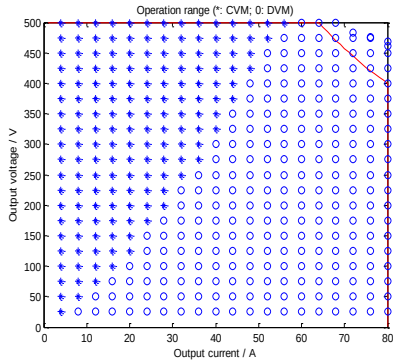

Fig. 6: Operation modes the whole operation range of SPRC-LC with parameters of Table 2

Table 2: Optimized SPRC-LC parameters

Passive component	Commutated parameter	Implemented parameter
$n = N_2 / N_1$	9 : 10	9 : 10
L_s	49.068 µH	46 µH
C_s	482 nF	484 nF
C_p	214.2 nF	220 nF
L_{out}	120 µH	120 µH
C_{out}	32.8 µF	33 µF

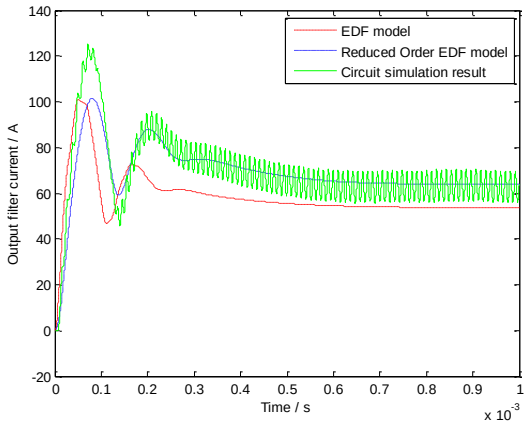

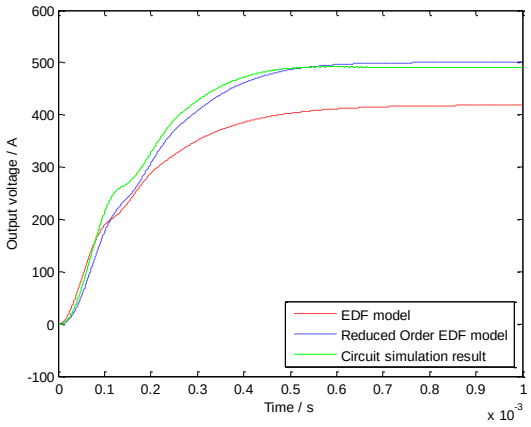

Fig. 7: Comparison results at the operation point 500 V / 64 A (DVM)

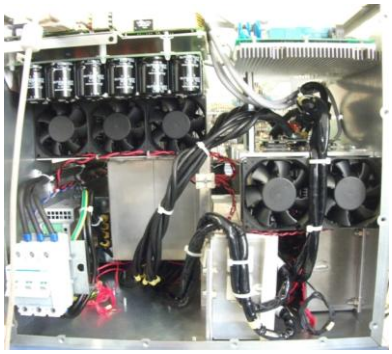

Fig. 8: SPRC-LC demonstrator

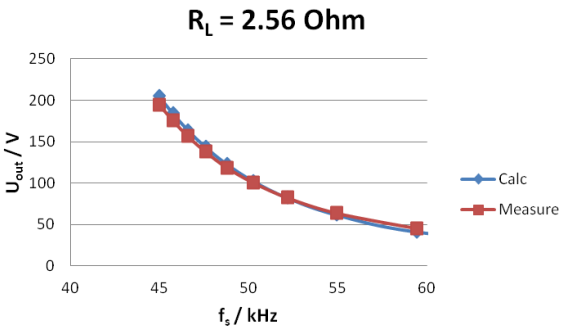

Fig. 9: Validation of the control characteristic

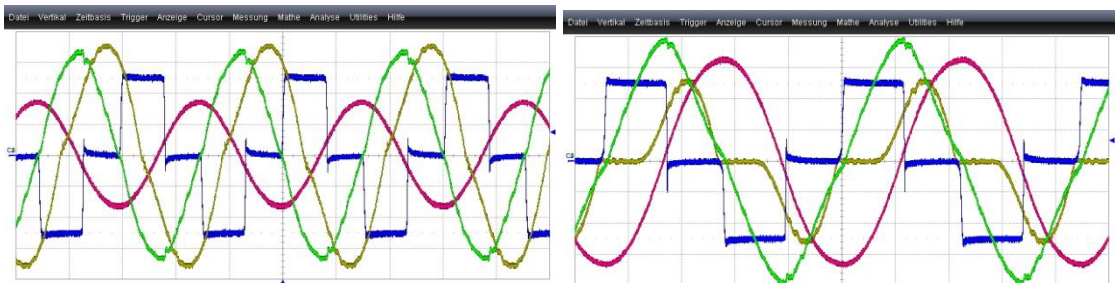

Fig. 10: Measured output voltage of full bridge (blue), resonant current (red), voltage on C_s (green) and C_p (yellow) in CVM (link) and DVM (right)

Bidirectional HVTS (WP 2.1.5, WP 4, WP 5)

Overview and objectives

Testing of buried high-voltage cables becomes more and more important for reliable power grids. The VLF (very low frequency) 0,1Hz technology allows testing of high-voltage cables with much less energy due to a lower test frequency. But, it requires more technical test equipment. BAUR established this technology during last years. However the current technology is limited by power dissipation, scalability and weight.

The RPC-HVTS-DCS project aims to solve the challenges by development of a **bidirectional high-voltage converter**. A four quadrant high-voltage source is able to reduce power dissipation to a minimum. Energy that is used to load the capacitive cable to its maximum voltage can be fed back to an energy storage during unload of the cable. The polarity changes and the cycle restarts.

For verification and demonstration purposes a demonstrator is developed and built that eliminates the disadvantages of the current technology.

Today's technology

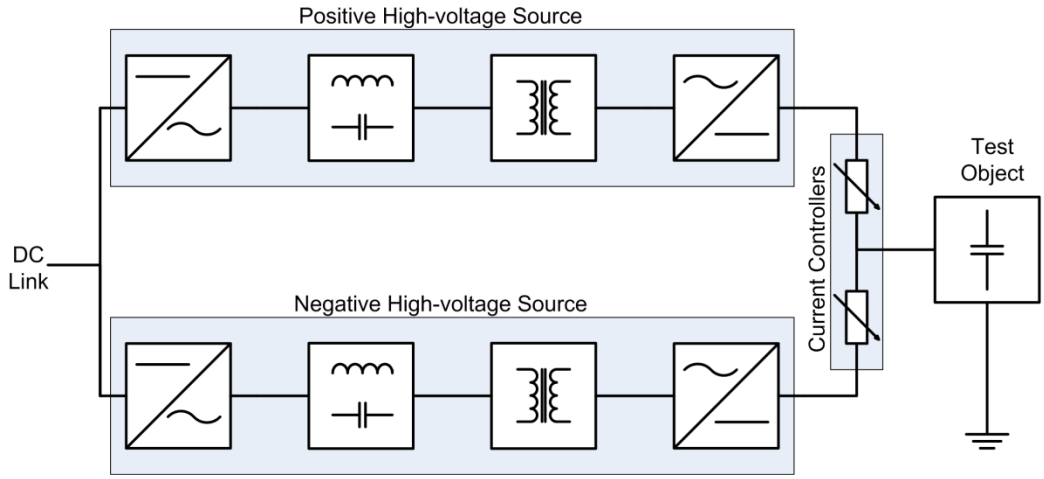

Figure 1: Block diagram of today's VLF generators

Today's VLF generators are built as shown in Figure 1. Two separate high voltage sources for each polarity load the capacitive cable through the current controllers. The current controllers consist of cascaded transistors with a direct current control. During unloading of the cable the energy stored in the cable will be dissipated in the current controllers. Since the current controllers are high-voltage components they are placed together with the high-voltage sources in a high voltage tank built of steel or aluminum. The tank must be able to dissipate the heat generated in current controllers. These facts result in heavy generators. If the energy stored in the cable could be recycled to the low-voltage side (back to the DC link) it could be stored for the next test cycle. This is the goal for the HVTS bidirectional part in project RPC-HVTS-DCS.

Research on bidirectional HV-converter structures (D2.1.3a, b, c)

Known high- to low-voltage converters are used in high-voltage direct current transmission. Due to its extreme high power ratings this technology is not applicable for VLF generators. VLF generators need a small converter facilitating high voltage but at low current. For this reason different power converter schemes were evaluated for use in a high-voltage environment. For the selected topologies fundamental harmonic analysis (FHA) were performed. Further on time-based simulations verified the FHA. The best suitable topology was taken to design a novel bidirectional high-voltage four quadrant source.

Research and development of HV-components (D4c, D5a,b,c)

Since the novel bidirectional topology differs completely from today's VLF generators a variety of new components and functional blocks had to be designed and tested. This relates to all components placed in the high-voltage tank. Firmware had to be implemented in a few microcontroller based boards for control and measurement purposes. Even a new high-voltage tank was designed after mechanical design studies performed by a CAD system showed its advantages compared to the current VLF generators. The result is shown in Figure 2.

Figure 2: Bidirectional HVTS demonstrator

Initial start-up and tests (WP6, D6)

Step by step the initial start-up of the demonstrator has been performed. At first the communication firmware for the microcontrollers has been tested. All actuator and sensor signals are processed by a DSP-system. The four quadrants of the voltage-current diagram were extensively tested at characteristic steady states.

U_{HV} in kV	I_{HV} in mA	U_{ZK} in V	I_{ZK} in A	P_{in} in W	P_{out} in W	η in %
10	1,4	93	0	14	0	0%
10	5	39,6	0,89	50	35	70%
10	10	36,8	2,11	100	78	78%
10	15	34,9	3,32	150	116	77%
10	20	33,1	4,5	200	149	74%
10	25	31,2	5,77	250	180	72%
10	30	29,5	6,94	300	205	68%
10	35	27,7	8,14	350	225	64%
10	40	25,7	9,45	400	243	61%

Table 3: Results of high- to low-voltage conversion tests

The results of the high-to low-voltage conversion tests are shown in Table 3: Results of high- to low-voltage conversion tests. An external high-voltage power supply was used to feed a constant voltage of 10 kV to the bidirectional converter. Through variation of the load on the low-voltage side different power points of the converter could be tested. A maximum efficiency of 78% was reached as compared to zero of the current solution.

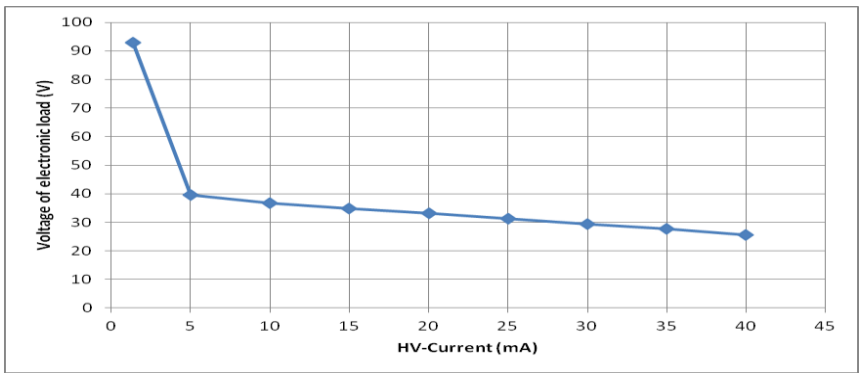

Figure 3: Voltage of electronic load at 10 kV in dependency of HV-current

Based on the properties of the chosen converter type the relation of the input to the output voltage should be constant. Figure 3 shows that the output voltage depends of the HV-current. This can be explained by the resulting equivalent resistance.

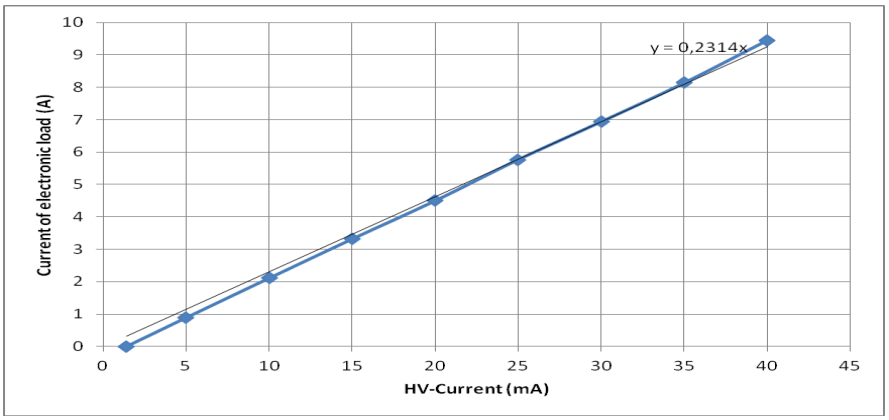

Figure 4: Current of electronic load at 10 kV in dependency of HV-current

In spite of the non-linear behavior of the output voltage versus HV-current the output current is nearly linear-dependent of the HV-current. The gradient in Figure 4 implies the conversion ratio of the selected converter type. This relation is used for the control structure to generate a sinusoidal high-voltage output voltage.

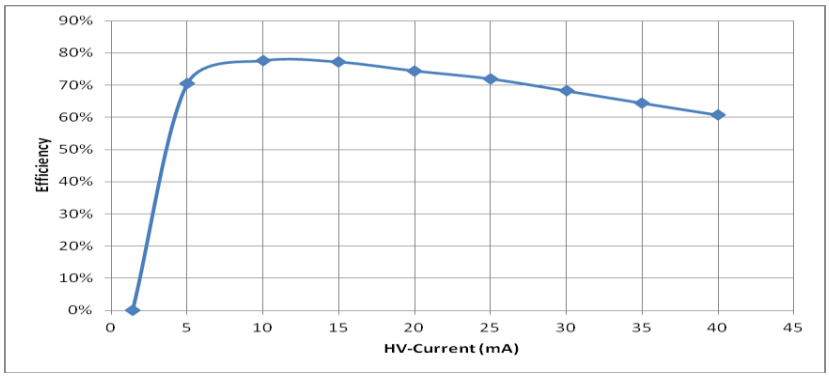

Figure 5: Efficiency of the convert in dependency of HV-current

The dependency of the HV-current on the efficiency shows Figure 5. A maximum efficiency of 78 % was attained at a high-voltage input current of 10 mA. At a lower input current the voltage-depending losses dominate. At higher input currents the resistive-depending losses dominate. The efficiency can be increased by a better selection of components. For this demonstrator only standard components were used.

Tests with VLF output (WP5, WP6, D6)

Initial tests have been conducted with controls being implemented in the DSP to enable the output of a sinusoidal 0,1Hz test voltage. The tests have been performed with a 600 nF capacitive load. The result is shown in Figure 6. The red line is the voltage at the test object. Its maximum is at about 10 kV. This line is almost sinusoidal. The current (green) has some deviations to the desired current (blue). Shown deviations can be minimized by improvements of the control strategy.

Summary

A novel bidirectional four-quadrant high-voltage converter was developed. A demonstrator has been built to verify the investigation. This technology enables BAUR to reduce power dissipation and thereby the goals of reduction of size, weight and costs are met.

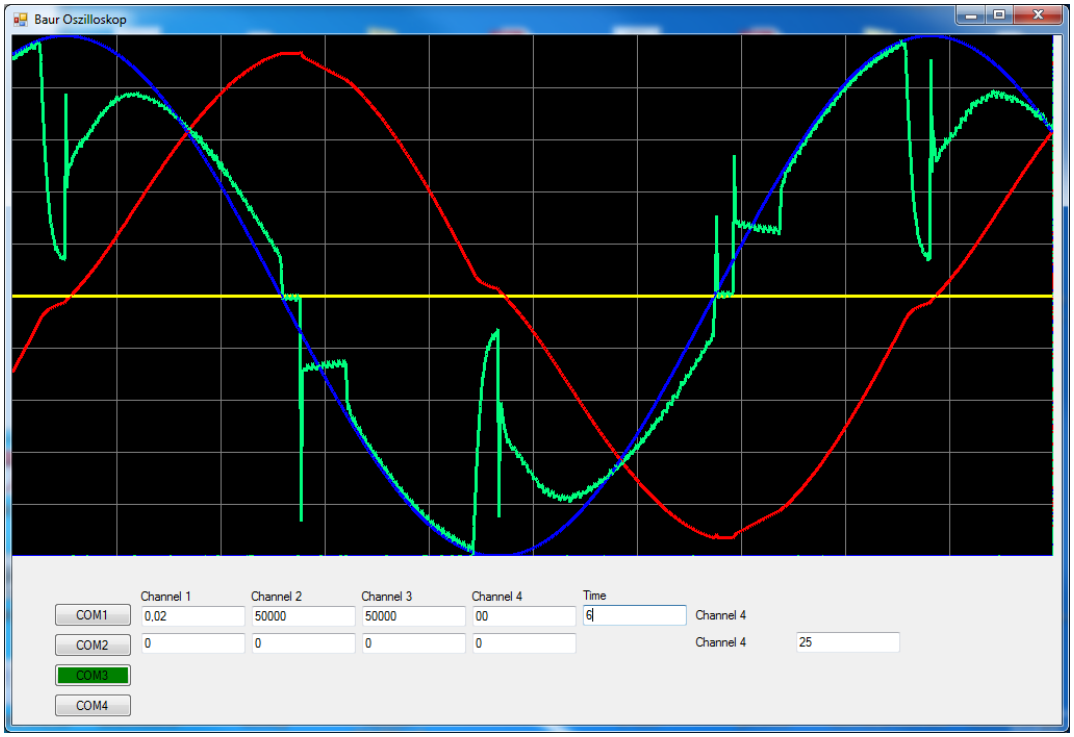

Figure 6: Output of an almost sinusoidal test voltage (red), output current (green), desired current (blue)

WIT

Parasitic models for the magnetic components used in the HVTS and DCS applications were envisioned for this work package.

Capacitance models

The presence of very high voltages and the use of large numbers of turns to achieve large winding ratios, leads to a rise in the significance of the parasitic capacitances in the wound magnetic components

A literature survey of models for parasitic capacitance of wound components yielded no models suitable to accurately predict the parasitic capacitance of a winding based only on material, geometrical and constructional parameters. An investigation into the reason for this yielded the insight that the total parasitic capacitance is extremely sensitive to geometrical variations and constructional variations. This effect is compounded by the large numbers of turns required in high voltage applications. Normal tolerances in the material geometries (eg. wire diameter) alone, can easily lead to more than 40% variation in the predicted capacitance values. This effect was confirmed by extensive parametric FEM analysis.

Additional constructional tolerances, arising from process and material variations, compound this effect even more. This effect was again confirmed by extensive parametric FEM analysis. The wide variations

reported in the literature between experimentally measured values of parasitic capacitances and the values predicted by the proposed models, is hereby readily explained.

Only accurate knowledge about the exact geometrical placement of each wire-turn in the wound component will make accurate calculation possible. It is therefore impossible to derive an analytical model, based on only a small number of parameters, to accurately predict parasitic capacitance. An FEM approach for capacitance calculation where large numbers of turns per winding are involved is computationally too expensive to employ in an optimisation loop where repetitive evaluation is required.

The suggested approach to deal with this problem is to assemble samples from the same materials and employing the same construction methods as in the final components. From the samples coefficients can be derived that can be used to calibrate the published models.

Loss models

In all high-frequency switch-mode converters the high-frequencies currents lead to additional losses over and above the DC losses. This impacts the efficiency of the converters and gives rise to heating which requires additional cooling of the final product. Designers of such equipment are always seeking for simple analytic models that will correctly and accurately predict the losses under various operating conditions.

A literature survey turned up some promising methods. These were used to predict losses in various wound magnetic components. This was undertaken for various permutations on small (E-30 based) wound components. This included foil and solid-wire windings as well as transformer and inductor configurations with and without air-gaps in the core. The predictions from the models were validated experimentally and in many cases satisfactory correspondence was achieved. Analytical models were/preferred chosen because of their relatively low computational requirements. This is important as the intended application is to include the loss models in the overall optimisation loop. This comes at the price of accuracy due to approximations required to keep the mathematics tractable.

This was repeated on wound components for the prototype bi-directional converter. Again the analytically predicted losses were validated experimentally, under both high and low excitation conditions. For the cases where the magnetic components can be considered to be operating primarily as an inductor or a transformer, the models show satisfactory performance. For the cases where the component operates as transformer-inductor combination, i.e. more of a coupled inductor, then the simple analytic loss models are no longer very good and a different approach needs to be applied.

In such a case a 2-D finite element model approach should be applied to obtain a rough understanding of the complex field distributions and then this used to determine the eddy current loss in the windings.

The results are best summarised in the table below.

	Foil windings	**Litz wire windings**
Inductors with air gaps		Inductor Ls Empirical factor approach completed 2D magnetostatic FEM based outstanding

Transformers	HV transformer Tx Wide and low frequency approaches completed Undriven shield layer effect	HV transformer Tx Wide frequency approach completed
Transformers with air gaps	Inductor Lp 2D magnetostatic FEM based and air gap outstanding	Inductor Lp 2D magnetostatic FEM based and air gap outstanding

Suggestions for improved loss modelling are summarised in the previous table. With the increased processing power of modern computing devices it will in the future be feasible to do a simple 2D FEM analysis of a basic window cross section, in order to derive coefficients for analytical models. This will significantly enhance the accuracy of the loss predictions beyond what can be obtained from purely analytical methods.

Conclusion

The dependence of parasitics on second order parameters make them susceptible to dramatic variations when small changes in the underlying parameters are present. This is often brought on by the manufacturing tolerances of wires and isolation materials. To accurately model this requires an intimate knowledge of a large number of constructional parameters. This makes the models complex and computationally expensive if not impossible to evaluate. The proposed approach is to make use of experimentally determined coefficients for analytical models of parasitic capacitances. For losses the use simple 2D-FEM analysis of the magnetic distribution in a window cross section is recommended to determine coefficients for analytical loss models, where simple approximations no longer hold.

HNI

Within the work package WP 3.1 the following results were achieved:

a. The worldwide market volume at a voltage level from 150-250 kV is relatively low: about 100.000 km cable run in the ground. At a voltage range beyond 50 kV the market volume is much higher: in this range about 500.000km cables are in the ground worldwide. These high voltage cables are mainly tested with resonance testing equipment which is sold for approximately 800.000 EUR. A test including the personnel costs, the mounting and dismounting of the device is offered by KEMA or IPH Berlin (service providers) for about 20.000 EUR. The resonance testing equipment enables to test cables up to 200 kV with each of these devices. Typical tests of high-voltage power lines (110 kV) with resonance testing equipment: In factory at 3 x U_0; after construction at 2,5 x U_0; tested cable length vary between 40 m and 11 km.
b. The regional distribution of the worldwide high and extra-high voltage power lines is shown in fig. 1.

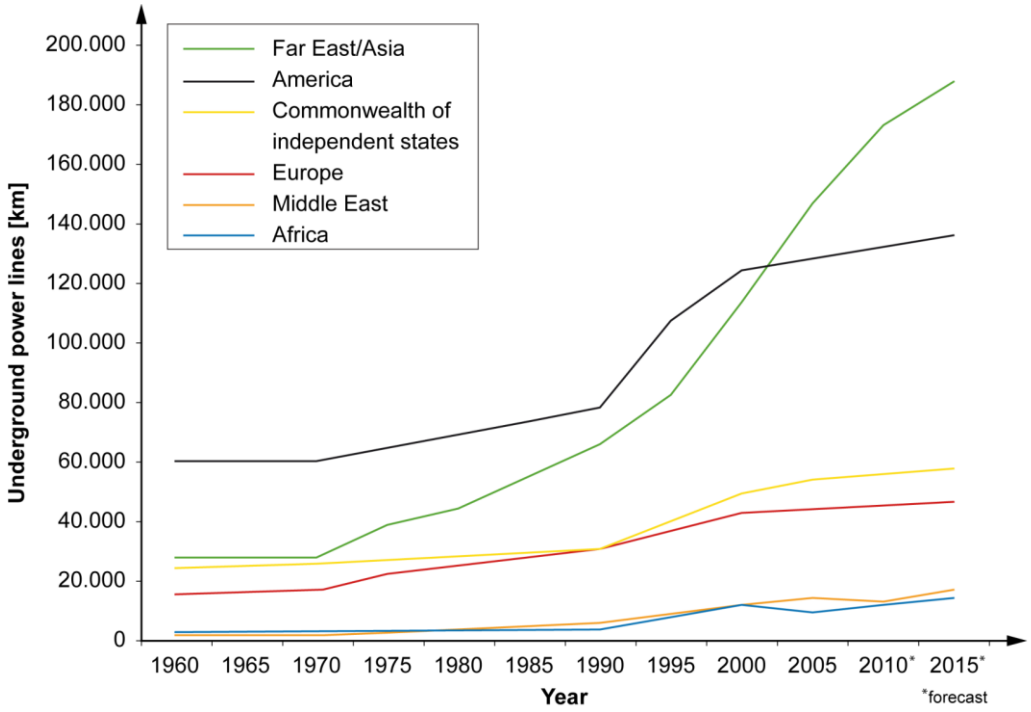

Fig. 1: High voltage underground power lines (50 to 163 kV)

The largest markets for the HVTS business are therefore located in Far East/Asia and America – followed by the Commonwealth of Independent States and Europe with a considerable margin. Far East/Asia and America own the most high-voltage cables. In addition to that they are also still most active at building new ones.

c. Nine resonance testing equipments (technology to be substituted) are in use in Germany, two in the USA and two in Switzerland. The USA has the most Distribution Network Owner (2440) followed by Germany (950) and Switzerland (800). The owners are all potential buyer of HVTS-VLF technique. In this overview china is missing because of its centralized organization and structure.

d. The competition analysis focuses on three market segments which are important in respect to the HVTS technology for the considered company. These are the market segments cable fault detection (CFD), cable testing and diagnosis (T&D) and services regarding cable testing (service cable). The companies which were part of the competitors' analysis are differing a lot concerning their regional appearances and their market performance portfolios. C1 and C2 are the current main competitors in the business area of cable fault location and testing and diagnosis. Half of the competitors are expected to increase their degree of competition.

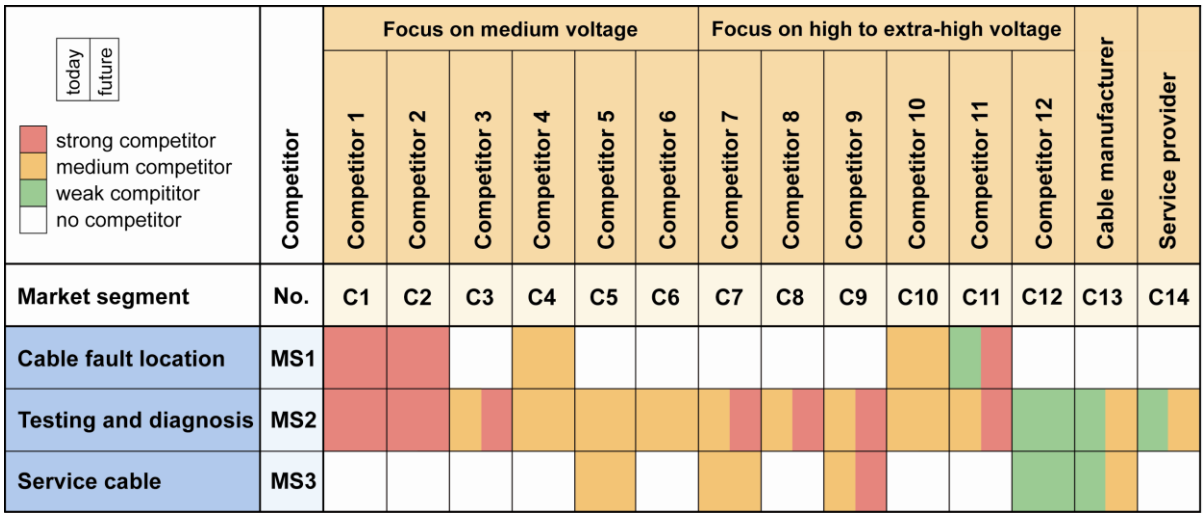

Fig. 2: Overview about current and upcoming competitors in relevant market segments for the considered company (anonymized)

e. The two competitors C13 and C14 are groups of companies: C13 covers cable manufacturers and C14 includes service providers. These groups are considered because these companies could expand their business and become strong competitors. Companies manufacturing resonance testing units will become competitors when the HVTS-VLS technique is ready for the market.

f. A useful method to visualize trends is a trend radar (fig. 3). Altogether 24 relevant trends were identified. The trends with the highest probability of occurrence and impact on the energy industry are “Smart grids”, “E-Mobility”, “Electricity from renewable energy” and “Availability of resources”.

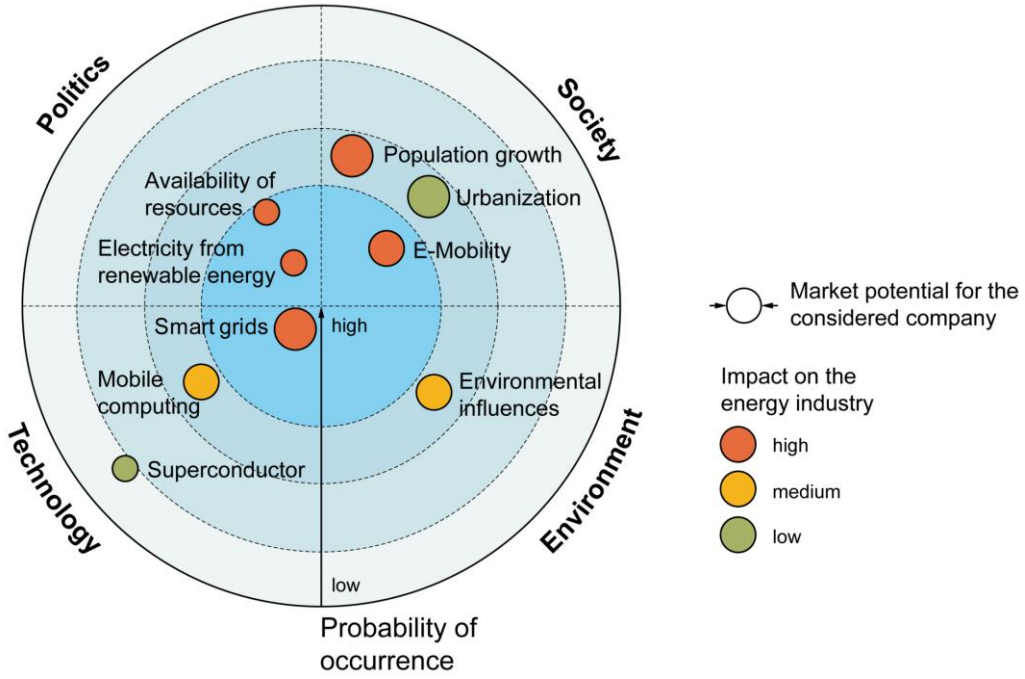

fig. 3: Trend radar for the future of cable testing (extract)

g. Regarding test and diagnosis using the VLF technique voltage levels of approximately 130 kV have been approved. Generally VLF tests and diagnostics are practicable from 69 kV as there are no standards or

restrictions. The regarded company could be a pioneer in this section and could set the standards based on their own competences.

h. The result of the trend and technology mapping shows, that the HVTS VLF technology has a good chance to be a market success. Using the list of requirements, the considered company is qualified to develop a promising product.

List of requirements	req./wish
Construction size: Should fit into a regular transporter	r
Weight: Considerably less than the permitted payload of a transporter	r
Voltage range: Up to standard high voltage levels	r
Field of application: Primarily urban areas	r
Kind of output voltage: Pure sinus wave (AC)	r
Time for setup: Less time than a resonance testing equipment	r
Time for measurement: Less time than a resonance testing equipment	r
Recovery of energy: Energy should fed back into the grid	w
Price: Much cheaper than a resonance testing equipment	r

fig. 4: List of requirements for high volt test systems with very low frequency

For work package WP 3.2 the following tasks have been completed:

a) Above all, for the power units next generation new scopes of application were identified.

b) Creativity techniques were used within workshops to identify ideas for “diversification”.

c) A portfolio “benefit for the customer” to “effort for the regarded company” is the result of a systematic idea- and innovation-management process. We used this method for instance to structure new requirements for the power units in order to widen the scope of application: